Microplastics in Antarctica - a Plastic Legacy in the Antarctic Snow?

Kirstie Jones-Williams
British Antarctic Survey
Sebastian Primpke
Alfred Wegener Institute for Polar and Marine Research https://orcid.org/0000-0001-7633-8524
Tamara Galloway
College of Life and Environmental Sciences, University of Exeter, Exeter EX4 4QD, UK
Emily Rowlands
emirow@bas.ac.uk

British Antarctic Survey
Matthew Cole
Plymouth Marine Laboratory https://orcid.org/0000-0001-5910-1189
Claire Waluda
British Antarctic Survey
Clara Manno
British Antarctic Survey

Article

Keywords:

Posted Date: October 2nd, 2023

DOI: https://doi.org/10.21203/rs.3.rs-3389603/v1

Additional Declarations: There is **NO** Competing Interest.

MICROPLASTICS IN ANTARCTICA - A PLASTIC LEGACY IN THE ANTARCTIC SNOW?

Authors: Kirstie Jones-Williams, Sebastian Primpke, Tamara Galloway, Emily Rowlands, Matthew Cole, Claire Waluda, Clara Manno (clanno@bas.ac.uk)

Key words:

Abstract

Microplastic pollution in remote inland Antarctica is largely unknown. This study explored the plastic footprint of snow from remote Antarctic camps; Union Glacier, Schanz Glacier and the South Pole. Refined automated FTIR techniques enabled interrogation of <25 µm microplastics and fibres in Antarctic snow for the first time. Microplastics were pervasive (73 - 3,099 MP L^{-1}). The majority (95%) measured <50 µm, indicating that previous microplastic reports in Antarctica may be underestimated, due to analytical restrictions. Polymer composition and concentration did not vary significantly between sites, with dominant polymers being polyamide (PA), polyethylene terephthalate (PET), polyethylene (PE) and synthetic rubbers, likely from both local (clothing, ropes, flags) and long-range (aerially deposited) sources. Results indicate that even in the most remote regions of earth, humans are leaving a plastic legacy in the snow, and illustrate the importance of remote, cryospheric regions as critical study sites for determining temporal fluxes in microplastic pollution.

Introduction

Antarctica is regarded as the world's last great wilderness. Isolated by the Antarctic Circumpolar Current (ACC), it exists as the coldest, driest, highest, and most remote continent on planet earth. The frozen continent has unique protection under the Antarctic Treaty System (ATS), effective since 1961 (Secretariat of the Antarctic Treaty, 2023). Human presence in Antarctica is therefore limited to scientific research, fishing, tourism, and support for logistics with any proposed activity undergoing an environment impact assessment. Despite environmental provisions, Antarctica is not immune to anthropogenic pressures. The ACC, once considered a physical barrier for pollution and invasive species, can be breached, bringing pollution to Antarctica via ocean currents (Sul et al., 2011; Fraser et al., 2016). Long range atmospheric transport may also be a key mechanism for microplastic transport from populated to remote regions (Dris et al., 2015, Bergmann et al., 2019) or from the ocean (Allen et al., 2019) to remote regions including Antarctica (Avez et al., 2022). The polar regions are often considered a sink for pollutants (Van Sebille et al., 2020) via atmospheric and ocean currents, however global warming threatens the re-emergence of these contaminants from permafrost (Potapowicz et al., 2018) and sea-ice melt (Obbard et al., 2014).

The presence of humans as carriers of local pollution in Antarctica potentially puts this region at even greater risk (Shirsat et al., 2009; Cai et al., 2012; Reed et al., 2018). With most permanent research stations and tourist landings occurring on the coast (COMNAP 2022, IAATO, 2021), local point sources of pollution are understudied in the remote inland regions of Antarctica.

Plastics are a diverse group of polymer-based materials, which can be altered physically in the manufacturing process (melting, extrusion, palletisation) and by incorporation of other chemicals (flame retardants, colorants, plasticisers). Once released into the environment, weathering processes will further alter the chemical and mechanical properties of the plastic and once below 5mm in size, these so-called microplastics constitute a vast and diverse range of pollutants (Thompson et al., 2015). Whilst environmental policies determine that all plastics must be removed from the Antarctic after use, there currently lacks any mention of microplastics in this environmental framework (Annex III, Madrid Protocol).

The single study thus far of Antarctic snow (from Ross Island, East Antarctica) used visual identification, followed by micro-Fourier transform Infrared spectroscopy (µFTIR) to identify an average of 29 particles L^{-1} in snow (Aves et al., 2022). As well as localised sources of pollution from the nearby research stations (Scott base and McMurdo station), long-range transport of microplastics from up to 6000 km across the continent was determined using a backward trajectory air-mass model. Methods used were limited for microplastic detection for sizes > 50 µm. However, microplastics < 50 µm have been identified as a major component of plastic pollution in other remote regions in the Arctic (Peeken et al. 2018, Bergmann et al., 2019). The footprint of humans in Antarctica may therefore be much greater than current estimates.

The current study measured concentrations of microplastic down to 11 microns in sub-surface snow estimated to represent the snow fallen in the year previous (Lazzara et al., 2012; Hoffmann et al., 2020). Samples were taken from three different remote camp sites located in Antarctica (Union Glacier, Schanz Glacier and the South Pole). The camp at Union Glacier is seasonal and is operational during the summer period between October/November and February, hosting approximately 420 people annually, housing up to a maximum of 140 people at any given time IAATO, (2021). At Schanz Glacier there is a small touristic “retreat” camp which houses a maximum of 16 people. In contrast, at the South Pole, the National Science Foundation (NSF) centre, houses a maximum of 100 people in the summer with approximately 50 people overwintering, with approximately 250 people visiting the centre each year.

Since its first introduction in the 1950s, there is now enough plastic pollution to form a permanent and distinct layer in the earth's fossil record (Zalasiewicz et al., 2021). But with comparably low visible plastic pollution in Antarctica, little is known about this plastic legacy on the frozen continent. This study provides new insights into the presence of plastic pollution in the most remote, inland sections of continental Antarctica by measuring microplastics <50 µm to test the hypothesis that microplastic reports from earlier studies in Antarctica are underestimated due to analytical restrictions.

Methods

Field Collections

Snow samples were taken from three different locations in Antarctica (Union Glacier, Schanz Glacier, and the South Pole) (figure 1). Union Glacier (79°460 S, 83°240 W) is situated at the northern edge of the Western Antarctic Ice sheet, the glacier drains through the Heritage Range, Ellsworth Mountains, and extends 86km up to the grounding line of the Ronne-Filchner Ice Shelf. Sitting approximately 550m above and draining into Union Glacier is the similarly u-shaped Schanz Glacier. The Amundsen-Scott Base and field camp is 600 km away from Union Glacier (figure 1). These three sites represent three different remote camps, varying in size and accessibility (table S1). Twelve sites were selected for analysis: five at Union Glacier (UG1-UG5, close to the downwind of the camp), four at Schanz Glacier (SG1-SG4, 2km area between the tracks and the retreat), and three at the South Pole (SP1-SP3, one at the runway, and two at 250m intervals in the direction of the westerly prevailing wind). A control sample was taken from the most remote location accessible (figure 1, C1), atop an exposed ridge between the Schanz and Driscoll Glacier.

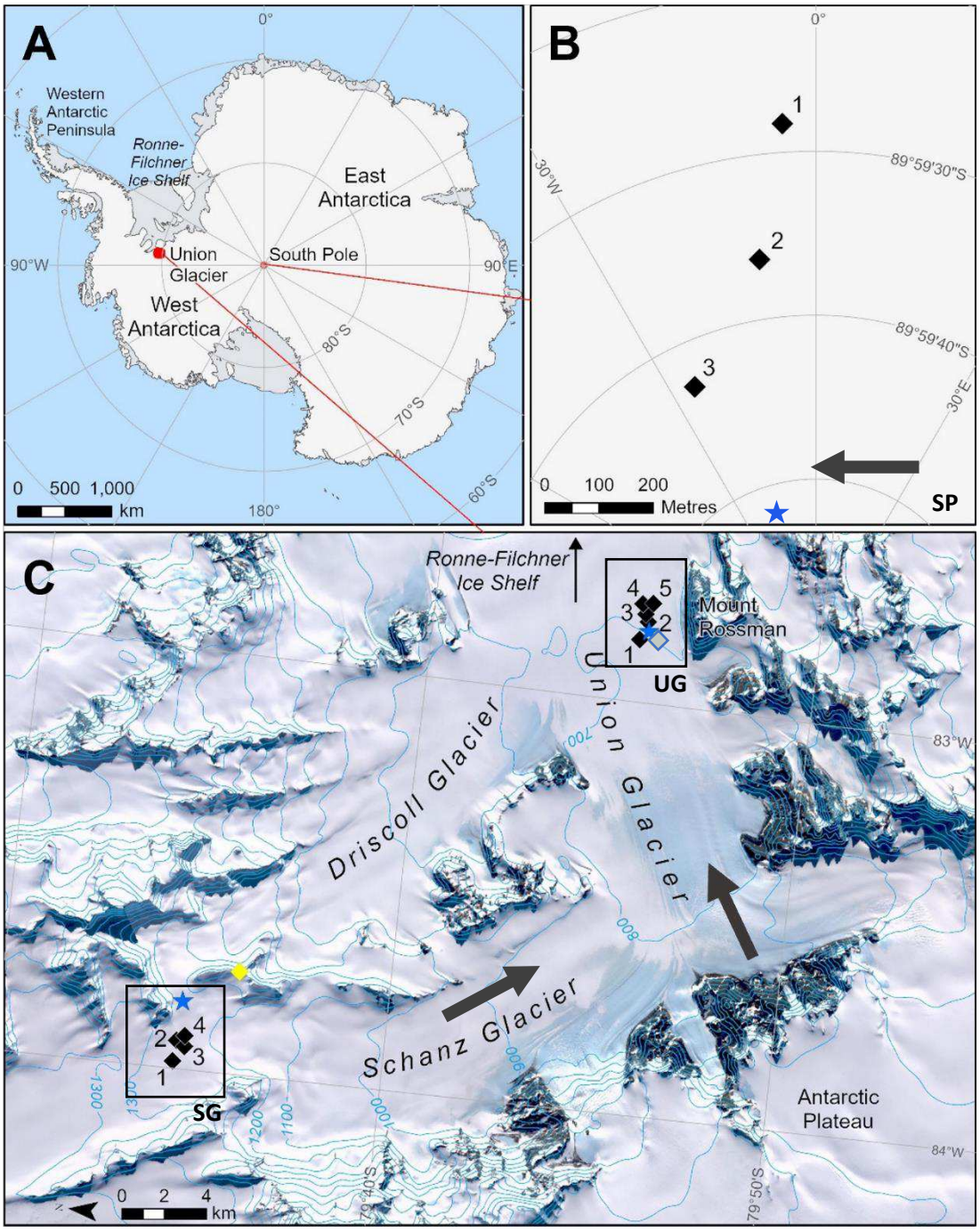

Figure 1 Locations of the study regions relative to one another in continental Antarctica (A), and the individual sample locations at B: the South Pole (SP) and C: Union Glacier (UG) and Schanz Glacier (SG). Arrow in B represents the prevailing wind direction. Arrows in C represent the drainage direction of each glacier. Blue stars mark the camps. Samples are marked by black diamonds. Control sample taken near Schanz Glacier is denoted by a yellow diamond. Grey diamond to denote location of "clean snow" as referenced in field collection methods. Maps were compiled in Quantum GIS (v3.10.4). Background image (C) was extracted from the Landsat Image Mosaic of Antarctica (LIMA). Coastline and contours from the SCAR Antarctic Digital Database, accessed 2023. Orange dashed line approximate location of ground penetrating rador (GPR) track near Schanz Glacier.

All three sites share the same snow accumulation rate, prevailing wind direction and annual precipitation. Additional environmental parameters and the proximity of each individual sample to the nearest camp were recorded to determine whether these variables had any statistical influence on the composition and concentration of microplastics. Temperature, wind speed and wind direction were recorded using a kestrel 5000 Environmental meter, whilst precipitation conditions were described in observer notes and elevation recorded from the GPS and corroborated with the use of topographical map data (SCAR Antarctic Digital Database). Approximate distances of proximity were measured using GIS (figure 1).

A shallow pit was dug using a shovel to 20-40cm depth, and the sampler was positioned downwind of the pit (figure 2). The farthest wall of each pit was then "cleaned" of any potential contamination from the shovel by scraping approximately 5-10cm of snow from the wall with a stainless-steel cup. The cup was acid-cleaned between each sample site. Snow samples were taken at between 20-40 cm depth, to include the variance of snow accumulation across all sites. Thus, this study assumes sampling of this layer comprises the plastic legacy of the previous 1-2 years (Hoffmann et al., 2020; Lazzara et al., 2012).

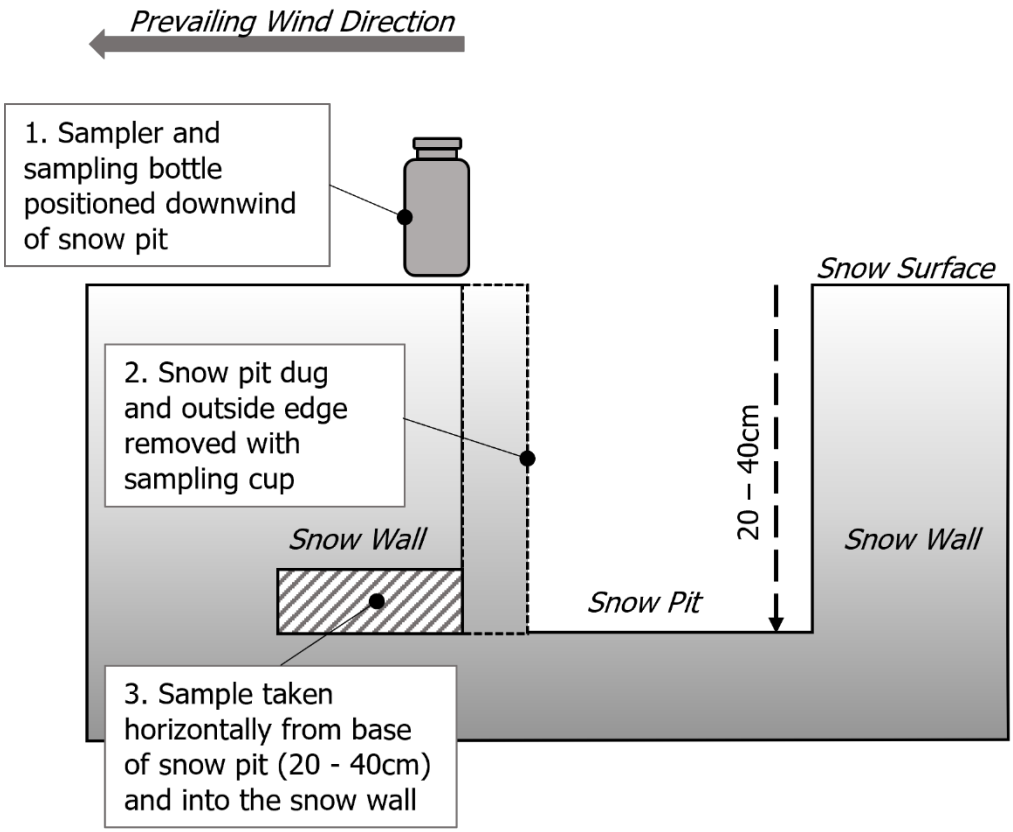

Figure 2 Schematic illustrating the sampling protocol.

A sample was taken by burrowing laterally into the side of the wall using the stainless-steel cup. The first "scoop" of each tunnel was discarded, with all subsequent collections with the cup decanted into an 800ml stainless steel tankard (ECOtanka™), which remained closed when not used and placed upwind of the sampler when being used. Each container was filled, bumping the base of the tankard to collect as much as possible, with variation in snowmelt volume recorded (table S1). Each tankard was then sealed and returned to the field laboratory for filtering.

In the field laboratory, samples were kept sealed and were slowly melted in the tankards. Once cooled, the snowmelt was weighed and then subsequently filtered through a 10ml funnel onto 25 mm diameter, 5 µm pore silver filters (Sterlitech) using a glass filter system, connected to a pump via polycarbonate tube creating a vacuum. All instruments were covered with aluminium foil when not being decanted for filtration.

The funnel was flushed through with "clean water" after filtering. In lieu of deionised water at the camp, "Clean water" was produced using the "clean snow" supply – an area of snow sectioned off, upwind of the camp (figure 1), used for generating the cooking water and shower water supply at Union Glacier. This snow was collected, and twice filtered through a 0.2 µm Isopore (polycarbonate) to remove any possible plastic contamination. Investigation under a stereomicroscope indicated that there was no visible microplastic or other particulate, as would be expected with passing through a small pore size filter. A sample of this "clean snow" was taken before filtering and processed as per other samples. The results of this are included in supplementary table S2.

Sample Processing

Samples were removed from the silver filter and transferred onto Anodisc® filters (Whatman®) (see SI 1) overlaid with a 2mm thick Barium Fluoride slide to analyse the whole filter area using Fourier Transform Infrared in transmission mode (Primpke et al., 2019).

Quality Assurance

In addition to the precautions already detailed in the sampling protocol, additional anti-contamination measures were taken in each laboratory (see SI 2). A contamination library was also built (see SI 3) and both negative and positive blanks were run (see SI 4)

Identification of Microplastics using Fourier Transform Infrared Spectrometry

Initial observations using an Olympus Stereomicroscope (figure 4A, D) indicated that MP particles were either less than 100µm or were MP fibres. This study combined the method of Primpke et al. (2019) with technical advice provided by Agilent Technologies; and used an Anodisc® filter with a 2mm

thick Barium Fluoride slide on top to press the material on the surface into the focal plane and to analyse the whole filter area using Fourier Transform Infrared in transmission mode.

All measurements were carried out using the Agilent 670 Fourier Transform Infrared (FTIR) spectrometer (Agilent Technologies, Santa Clara, CA), USA, with a cryogenically cooled mercury cadmium telluride (MCT) detector. The spectrometer was coupled to an Agilent 620 microscope with an automated XYZ-stage and 128 x 128 focal plane array (FPA) detector, cooled with liquid nitrogen. The FTIR system was continuously purged using a dry air generator (FGSR). The FTIR microscope was equipped with a 15 x IR objective lens and a 15-x visual objective lens. This stage held the sample in a bespoke filter holder enabling the transmission of infrared through the lower Cassegrain, the base of an Anodisc® filter where the sample was held, and through the Barium fluoride slide of the same shape and diameter as the filter. This setup facilitated FTIR imaging of both particles and fibres (Primpke et al., 2019, Roscher et al., 2021).

Filters were scanned in quarters, with each quarter measuring approximately 14mm x 14mm. The FPA detector enabled each quarter to be scanned, acquiring a mosaic of spectra (Primpke et al.,2017,

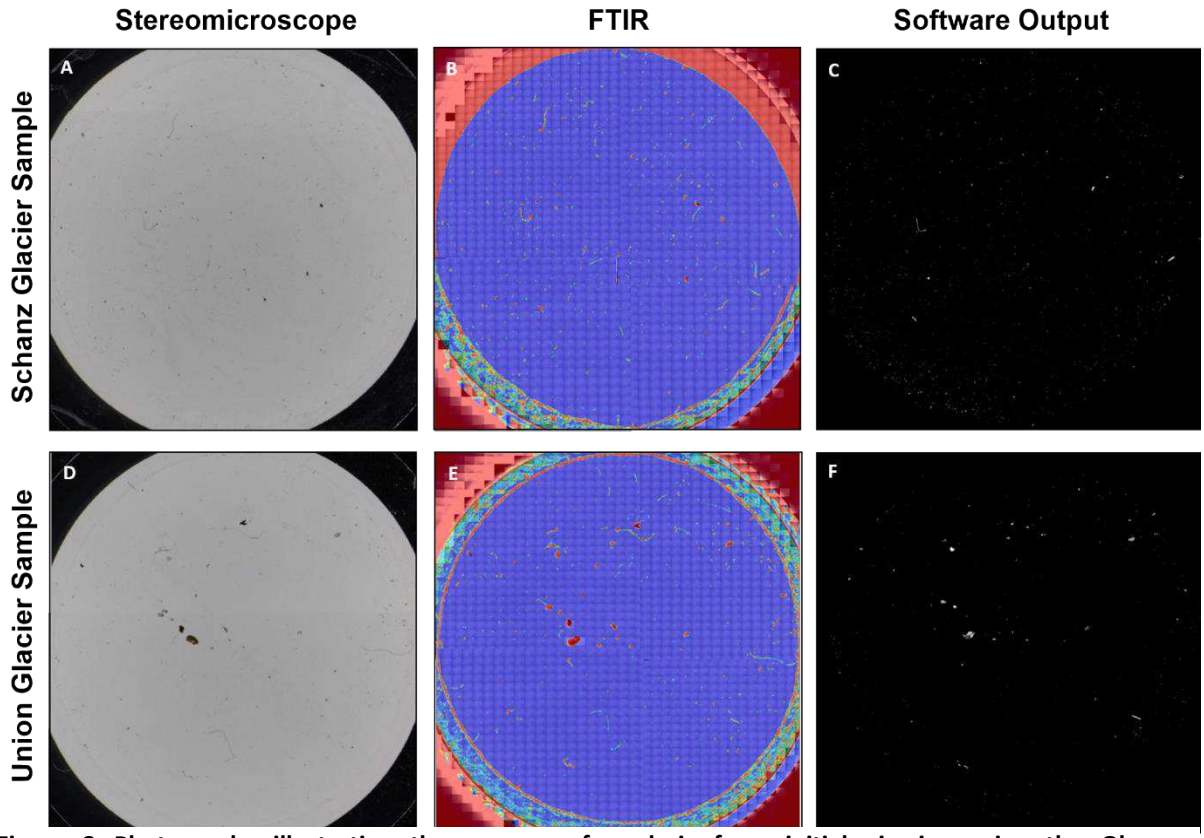

Figure 3 Photographs illustrating the process of analysis from initial viewing using the Olympus stereomicroscope (A, D), the original FTIR heat-maps (B, E) highlighting regions of infrared absorption (red) using the Agilent spectrometer and the final software output (C, F) having matched spectra to the reference library. The two sets of images (A-C, D-E) show two random samples; Schanz-Glacier-4 (SG4) and Union Glacier-5 (UG5).

2020a). This was calibrated with an XYZ stage allowing the exact coordinates at the end of the scan to be used to accurately identify the start of the next scanning area, covering the complete area of each filter (diameter of 25mm, area 625mm^2) (figure 4B, E). The collection of multiple mosaics meant each sample took approximately 13 scannable hours spread over 2.5 days.

The Resolution Pro software, inbuilt with the Agilent µFTIR setup, was used to collect 16 co-added scans of each filter with 8 cm^{-1} spatial resolution, binned at four intervals. Before each sample scan, a background scan was collected on the clean window in the same spectral range, comprising 64 co-added scans.

Data Processing and Analysis

The data was exported, and the x,y matrix of spectral data, with 5.5 µm pixel resolution for each spectra, were analysed according to Primpke et al. (2020a). The siMPle software (version 1.1.ß) combined with MPAPP (Primpke et al., 2019) enables the assessment of both particles and fibre-like microplastics. siMPle coupled with the Agilent FTIR, has been demonstrated to yield correct assignment rates (>95%) when compared with other systems (Primpke et al., 2020a). siMPle is available open-access (www.simple-plastics.eu). Pixels in the region of the Anodisc® polypropylene ring were removed from the final sample calculations, with polyethylene and synthetic rubber also oversaturated in this region and subsequently removed. Using the reference library of Primpke et al., (2018), each spectrum's raw spectra and first derivatives are then compared with the reference database, using Pearson correlation. If both spectra match the same polymer, the polymer is successfully assigned (Primpke et al., 2017). This library also contains FTIR spectrum of natural materials such as coal, charcoal, natural polyamides, cellulose, quartz, and chitin. Concentrations of these materials are also reported.

The average concentration of each polymer and morphotype (fibre, particle) in the full procedural blanks were subtracted from each sample concentration (figure 3, result 1). Concentrations are presented as both the extrapolated number of microplastics (MP) and mass of microplastics per litre of melted snow (MP L^{-1} and µg L^{-1} respectively) (Bergmann et al., 2019). MP includes both particles and fibres. Concentrations for mass (µg) are calculated as part of the output from MPAPP (Simon et al. 2018), using the calculated surface area and reference polymer density as previously published (Primpke et al., 2020b).

Statistical Analysis

Data were tested for normality using QQ-plots. One-way ANOVAs with Tukey's post tests were used to test for differences between (1) total microplastics, (2) individual polymer concentrations and (3) natural materials found at each site. To explore the possible compositional differences between sites,

the polymer diversity for each site was also calculated using Shannon – Weiner diversity indices (H'). Looking at the samples ungrouped, Kendall Tau correlations were used to test for artefacts of sampling and analysis, by examining correlation between polymer concentrations with (1) wind speed during sampling and (2) the corresponding laboratory blank concentrations.

Results

Microplastic in sub-surface snow

Microplastics were found in all samples, ranging from 73 MP L^{-1} at Schanz Glacier (SG2) to 3,099 MP L^{-1} at Union Glacier (UG2) (table S2), with an average concentration of 817 ± 310 (SE) MP L^{-1} amongst all samples. There was no significant difference between the concentrations at the three sites (ANOVA, F=1.125, p= 0.366) (figure 5a). Mean mass concentrations ranged from 3.6 ± 2.3 (SE) µg L^{-1} at the South Pole 32.2 ± 31.0 (SE) µg L^{-1} at Union Glacier. Similarly, there was no significant difference in the mass concentrations between sites (ANOVA, F= 0.496, p= 0.625) (figure 5c). Reporting the median instead there remains no significant difference between sites (Kruskall Wallis, p = 0.57).

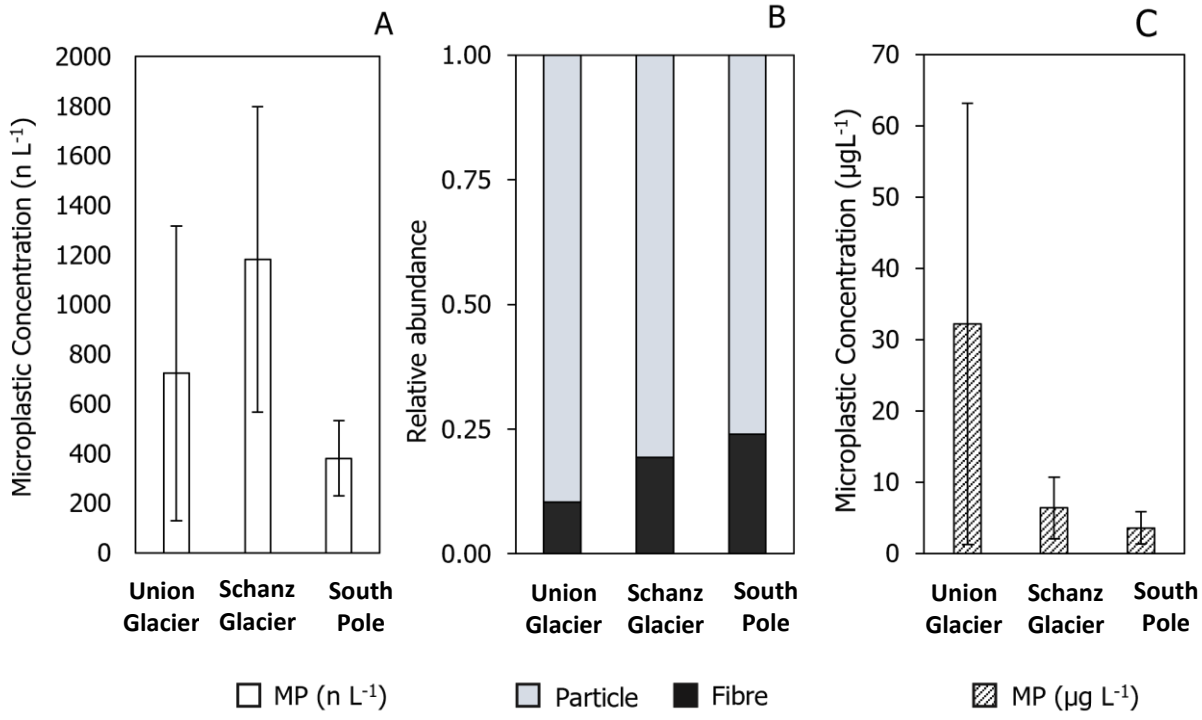

Figure 4 Comparison of average microplastic concentrations at each site. A: Average microplastic concentration and standard error bars for each site, recorded as normalised counts (n L^{-1}). B: Relative abundance of particles and fibres. C: Average microplastic concentration and standard error bars recorded as mass (µg L^{-1}).

Table 1 Summary statistics for Union Glacier (UG), Schanz Glacier (SG) and South Pole (SP) sites.

Statistic	Count Concentration (MP L^{-1})			Mass Concentration (µg L^{-1})		
	UG	SG	SP	UG	SG	SP
Minimum	84	73	152	0.34	0.57	0.16
Maximum	3098	2797	667	156.07	19.14	7.87
Median (SD)	152 ± 1328	929* ± 1232	322 ± 262	0.65 ± 69.26	2.93* ± 8.65	2.65 ± 3.94
Mean (SE)	723 ± 593	1182* ± 616	380 ± 152	32.19* ± 30.98	6.39 ± 4.32	3.56 ± 2.27

**Indicating the greatest concentration compared between sites using the same statistic and unit of measure*

Particles were the dominant shape, comprising 79% of total microplastics, whilst fibres made up only 21%. Particles were found in all samples; fibres were found in 11/12 samples (table S3). Comparing between sites, fibres comprised 24%, 21% and 19% in SP, UG, and SG respectively (figure 5B). There was no significant difference in the ratio of morphotypes between each site (ANOVA, F= 2.35, p= 0.15).

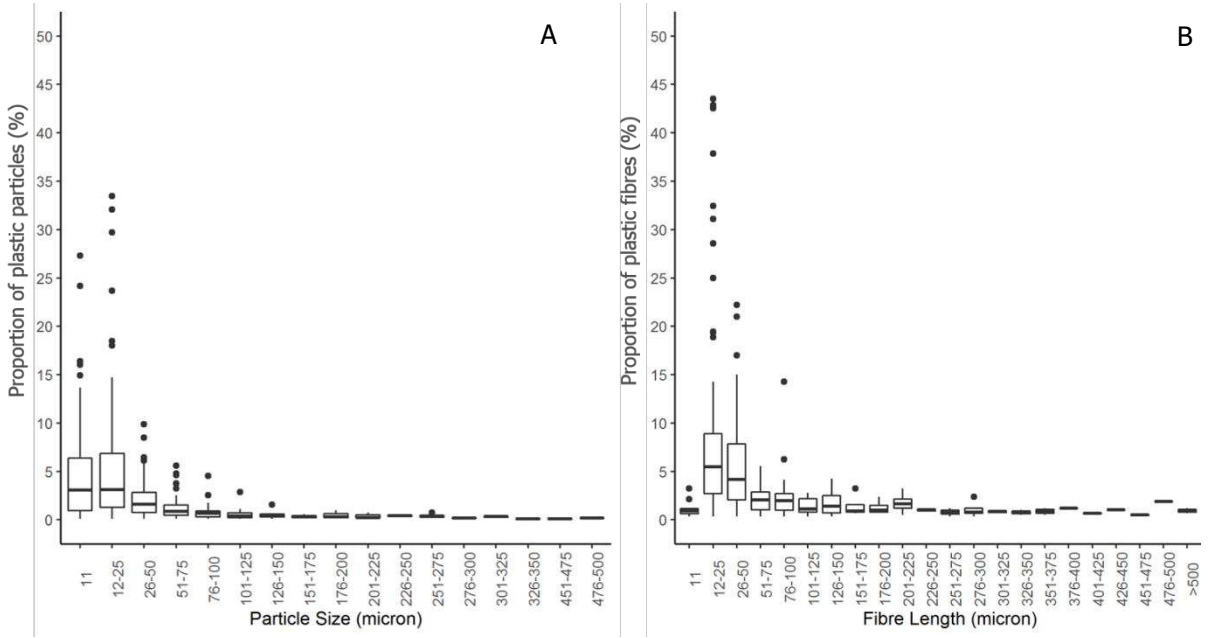

Figure 5 Box and whisker plots indicating the proportion of (A) microplastic particles and (B) fibres in different size classes across all samples. The upper and lower boundaries of the box denote the 75th and 25th percentiles, respectively with median bars and black points showing outliers.

The size of microplastic particles ranged between 11- 497 µm. Fibre length ranged between 11 and 979 µm. Size distribution was skewed towards the smaller size fraction with 95% of particles and fibres measuring less than 50µm (figure 6).

In total, 14 different plastic polymers were found. The most common polymer was polyamide (PA), comprising 55.5% of all microplastics found. This was followed by polyester (PET) (12.3%), polyethylene (PE) (10.9%), synthetic rubber (10.3%), acrylates/polyurethane varnish (4.6%), polypropylene (3.1%), chemically modified cellulose (CMC) (2.2%), polyvinylchloride (PVC) (0.4%), polystyrene (PS) (0.1%) and ethylene vinyl acetate (EVA) (0.2%). Other polymers (nitrile rubber, polycarbonate (PC), polycaprolactone (PCL), polylactic acid (PLA), polyoxymethylene (POM)) comprised the remaining 1.1%. There were between 2-10 different polymers found in each sample (figure 7). Highest polymer diversity was found at the South Pole (Shannon-Weiner Diversity, H' = 1.82), followed by Union Glacier and Schanz Glacier (Shannon-Weiner Diversity, H' = 1.47 and 1.04 respectively). The overall polymer composition between the sites was not significantly different (ANOVA F= 3.9, 0.99, p = 0.06).

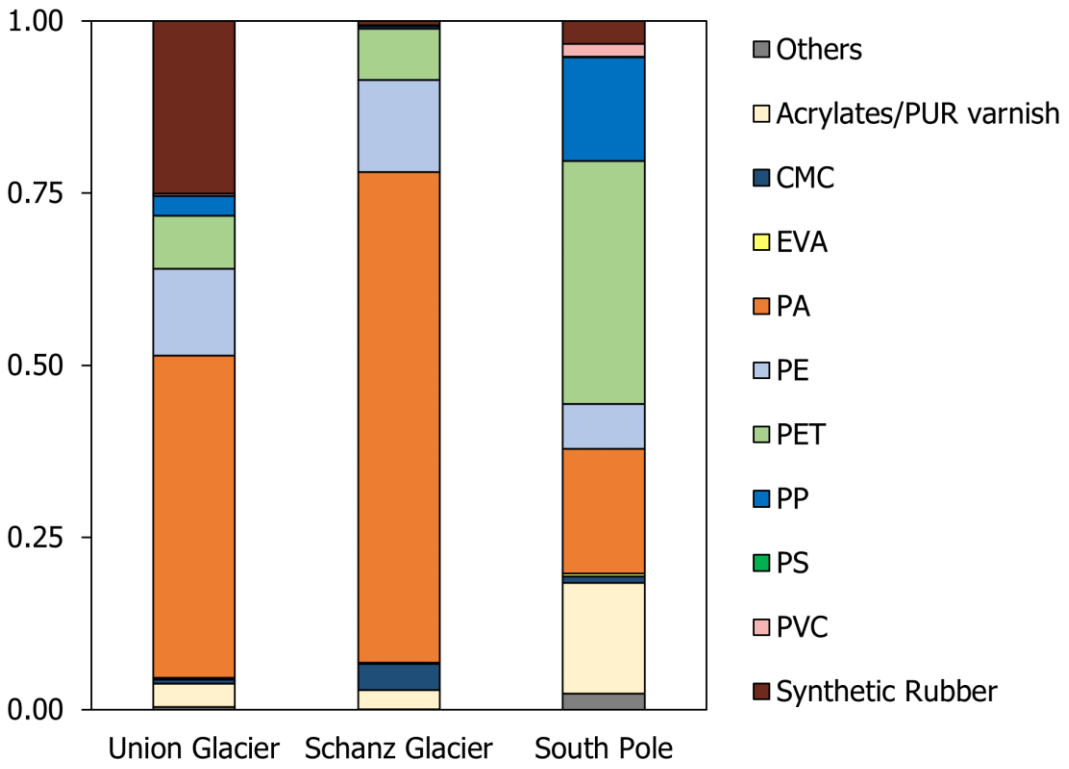

Figure 6 Stacked histogram showing average polymer composition of each sample accord to FTIR analysis. Others: (Nitrile rubber, POM, PC, PCL, and PLA).

Although there was no correlation between wind speed during sampling and overall microplastic concentration (Kendall Tau, p = 0.35), examining correlation for individual polymers, revealed a correlation between synthetic rubber concentration and wind speed on the day of sampling (Kendall Tau, p = 0.004) (table S7). Removal of this polymer had no significant effect on the overall sample concentrations and subsequent analysis.

Microplastics in the Control and technical replicates

Microplastics were found in the control sample, although the lowest recorded in the sampling campaign (30 MP L^{-1}). The control also had the lowest polymer diversity, with only POM (n=2) and PP (n=28) identified after normalisation, with all POM characterised as fibres and all PP as particles.

Two technical replicates were collected at the South Pole (SP3) (table S2). These two samples contained similar proportions of fibres (28% and 21%), compared with particles, but varied considerably in final concentrations, recording 181 and 460 MPL^{-1} in each. Polymer richness varied from 9 to 12, with EVA, PLA, and POM present in SP3b in very low concentrations (1.1% of total MP concentration). SP3a was dominated by PE (26%), PET (23%) and synthetic rubber (21%) followed by Acrylates (12%) and PA (11%). SP3a primarily comprised PA (26%), Acrylates (26%), PET (17%) and synthetic rubber (9%).

Other Material

In addition to plastic polymers, particles and fibres of natural origin were also found across all sites and samples, comprising 53%, 77% and 83% of total matter at Union Glacier, Schanz Glacier and the South Pole respectively (figure 8A). Concentrations were highest in Schanz Glacier (4060 ± (SE) 3342 n L^{-1}), followed by the South Pole (1887 ± (SE) 1662 n L^{-1}), and Union Glacier (808 ± (SE) 353 n L^{-1}), (figure 8B). These comprised plant fibres (natural cellulose), natural polyamides (furs), chitin, sand (quartz) and charcoal and coal (figure 8C). There was no correlation between the sampling parameters and the sample concentration (table S7).

Procedural Blanks

The average concentration of the full procedural blank was 240 ± 49 (SE) MP L^{-1}. Polyamides comprised approximately 27% of this total, followed by synthetic rubber (19%), and PE and CMC (13% each) (figure 9). Particles and fibres made up 75% and 25% of the total, respectively (table S5). The subtraction of both fibres and particles (Total microplastics) from each raw sample resulted in a reduction of between 22% (SG4) and 86% (SG2) (table 2). The laboratory blank comprised fewer microplastics, with an average of 125 ± 13 (SE) MP L^{-1} with the most common polymers being synthetic rubber (22%), polyamide (19%) and PET (17%) (figure 9, table S6). The laboratory blank comprised 89%

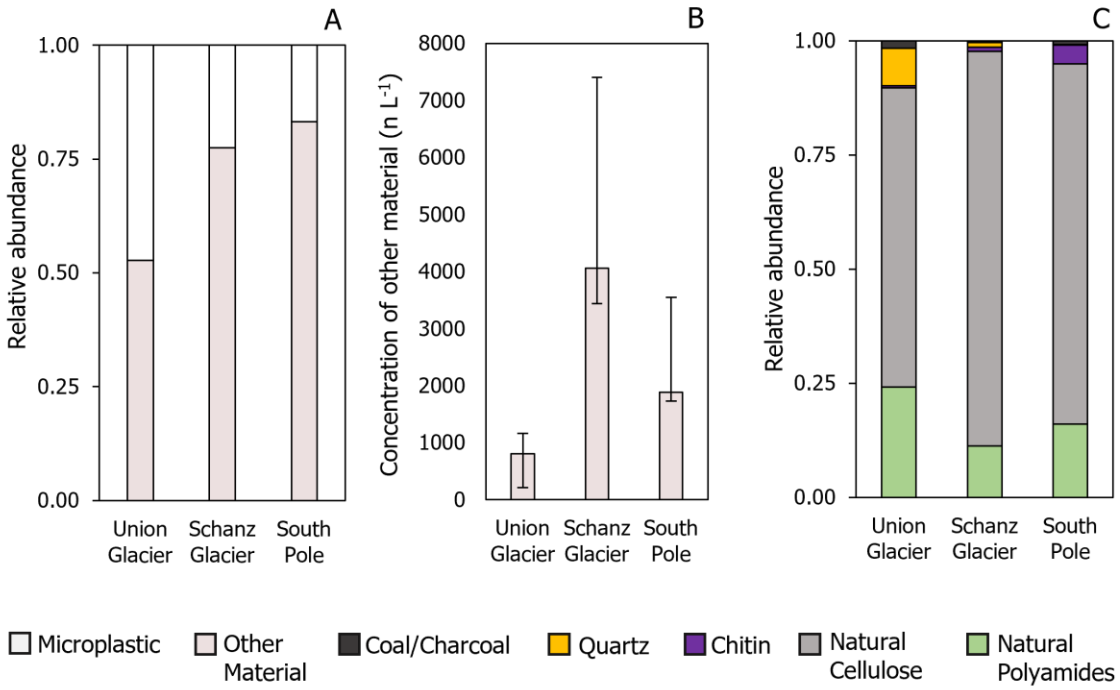

Figure 7 Comparison of other material at each site. A: Relative abundance of microplastics and other material. B: Mean concentration of other material at each site, with error bars indicating standard error. C: Relative abundance of the composition of other material.

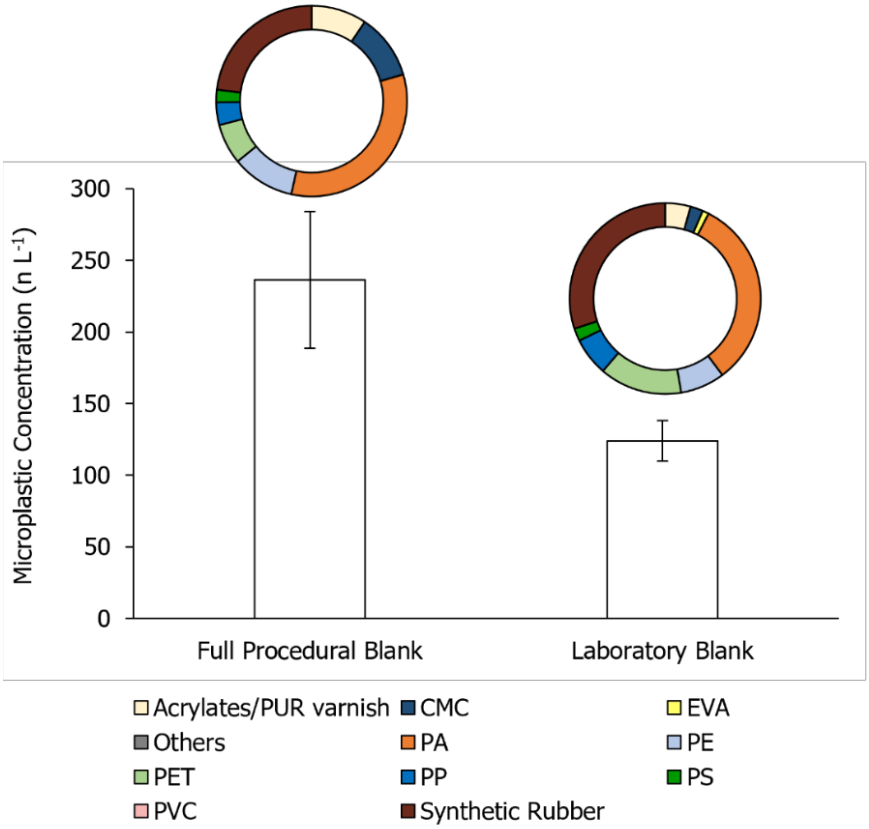

Figure 8 A bar graph showing the measured mean concentration of microplastics in the full procedural blanks and laboratory blanks, with ring plots above each to show polymer composition.

particles and 11% fibres. PVC and "other" polymers were absent from the blanks; however, a small amount of EVA (four particles in LB02) was identified.

Natural particles were found in all blanks, with 998 ± 100 (SE) particles L^{-1} were found in the full procedural blanks, comprising mostly of natural polyamides (55%) and natural cellulose (37%). Examination of the laboratory blanks individually shows an anomalously high concentration of natural particles and fibres in lab blank one (table S5). The remaining two laboratory blanks comprised natural polyamides (66%) and natural cellulose (25%), with an average total concentration of 558 ± 146 n L^{-1}.

Table 2 Raw microplastic concentrations and proportion of plastics in procedural blank yielding final MP concentration.

Sample	Total Raw (MP L^{-1})	Total Blank (MP L^{-1})	Normalised (MP L^{-1})	Blank Fraction (%)
SG1	875	489	56%	386
SG2	506	433	86%	73
SG3	2113	640	30%	1472
SG4	3575	777	22%	2798
SP1	633	480	76%	153
SP2	1293	628	49%	666
SP3	1666	1024	61%	642
UG2	4056	957	24%	3099
UG3	473	388	82%	85
UG4	606	441	73%	165
UG5	525	409	78%	116
UG1	543	392	72%	151
MS	158	128	81%	30
CS	1526	639	42%	888

Recovery Test

The results of the recovery test indicate that the transference step resulted in a 99% recovery rate (table 3). The subsequent estimate of concentration provided by FTIR analysis, indicated a loss of 4-5 nylon fibres. No correction factor was used based on these results.

Table 3 Recovery rates of three separate spiked samples containing different proportion of small and large nylon fibres.

	Starting Count	Fluorescent Count	Recovery Rate	FTIR Count

ID	Small	Large	Total	Small	Large	Total		Small	Large
1	87	3	90	86	3	89	98.8%	-	-
2	155	29	175	155	30	174	99.4%	-	-
3	112	35	147	110	36	146	99.4%	-	31

In the "clean snow" sample, 888 MP L^{-1} were found, comprising 76% and 24% particles and fibres respectively. Polyester (PET) was the main polymer, making up 32% of the sample, followed by PVC (26%) and Acrylates (17%). Three particles of acrylonitrile butadiene styrene (ABS) were unique to this sample compared to all other snow samples (table S2).

Discussion

This study refined the technique of automated FTIR analyses with additional methodology allowing for the analyses of fibres, often excluded from such automated analyses due to analytical restrictions. The average concentrations of microplastics collected from the snow, in regions of remote Antarctic camps was two orders of magnitude higher (817 particles L^{-1}) than a previous study (East Antarctica, near MacMurdo research station, average 29 particle L-1, Aves et al 2022). This is the first study to use automated FTIR imaging in Antarctic snow, enabling us to capture sizes down to 11 µm. This smaller size fraction has been shown to be the dominant fraction of microplastic sampled in the Arctic (80% measuring less than 25um; Bergmann et al., 2019). Average microplastic particle concentration in the current study was similar to Bergmann et al 2019 (625 particles L-1) who also found predominantly small microplastics particles (95% measuring < 50 µm) using automated FTIR techniques. Conversely, in the East Antarctic, Aves et al., (2022) manually sampled with µFTIR spectroscopy with a lower detection limit of 50 µm. We suggest that the size distribution of the particles shed light on the reason for the disparity between Aves et al, (2022) and the findings in this study. In fact, the concentration of microplastic observed in this study is reduced to 30 particles L^{-1} if only particles > 50 µm are counted. The method in the current study detected approximately 100 x greater concentrations using automated analysis, compared to Aves et al., (2022), highlighting how microplastic in Antarctic snow may be of greater concern that previously thought.

Particles were the dominant shape, comprising 79% of total microplastics in this study, whilst fibres made up only 21%. Conversely, Aves et at., (2022) found fibres were the most dominant microplastic morphotype (61 %) in Antarctic snow samples. Disparities are likely associated to the different analytical techniques (automated versus manual respectively) between the studies. In Arctic snow, whilst Bergmann et al., (2019) used similar automated techniques to detect microplastics down to 11 µm, they were unable to distinguish between synthetic and natural fibres, subsequently grouping all

fibres in microplastic counts, making it difficult to draw comparisons to findings in this study regarding microplastic morphology. However, in a study of microplastics in snowfall in a northern island of Japan, Ohno et al., (2023) determined particles heavily dominated the morphotype (97%) when using a lower microplastic detection limit of 30 µm. Like our findings, the smallest detectable microplastics were most commonly particles.

This study found polyamide to be present at all sites with the maximum recorded at Schanz Glacier (SG4: 2185 MP L^{-1}) where it made up 78% of the sample. Polyamide (including nylon) is mainly associated with textile fibres, and in these remote regions localised sources are likely to come from technical clothing, ropes and the flags which are used to guide safe accessible routes, laid out at the beginning of each season. The ubiquity of polyamide within the samples and absence from the control supports that this is a local source of pollution. Whilst Aves et al., (2022) also found Polyamide within samples taken from near McMurdo station in East Antarctica, it was not a significant proportion (6%). In the current study, the greatest polymer diversity was at the South Pole, which is the only permanent camp and may reflect a longer more persistent plastic footprint (Padha et al., 2022).

There was no significant difference between the microplastic concentrations across sites, despite the huge variability in term of human footprint at the different locations and no correlation was observed between distance from the camp and microplastic concentration. Conversely Aves et al, (2022) found that the concentration of microplastics measured at base sites (47 ± 8 particles L−1) was significantly higher on average than at remote sites (22 ± 4 particles L−1). This disparity could be due to the methods of Avez et al., (2022) potentially favouring local sources of microplastic pollution whilst the lower detectable size limit in this study allows more exploration of both local and long-range sources. For example, regional atmospheric models in other areas have shown that larger microplastics > 120 µm were likely from local sites whereas smaller plastics could efficiently be transported > 1000 km due to large surface area to volume rations and lower densities than surrounding dust particles (Long et al., 2022).

Recent atmospheric transport modelling indicates that Antarctica is a net importer of microplastics, with the flux of microplastics from mismanaged plastic waste in the ocean transferring to the atmosphere at the Antarctic coast likely exceeding anthropogenic sources of microplastics on the continent (Brahney et al., 2021). The dominance of small particles and fibres, particularly less than

100 µm in the current study indicates long-range transport as a means for deposition to remote locations (Bergmann et al., 2019; Zhang et al., 2019). Conversely the ubiquity of polyamide within the samples and absence from the control would suggest there are also local sources of pollution. Localised wind-driven snowdrift responsible for the redistribution of microplastics cannot be excluded. As an example, the current study observed highly localised microplastic concentration variation akin to the local variation in snow accumulation in this region (Hoffman et al., 2020) resulting from near-surface winds (Picard et al., 2019). The relationship between microplastic's size and their atmospheric residence time and deposition are still for the most part poorly understood. To determine whether microplastics in Antarctic snow are driven by local sites, by long-range transport, or a combination of the two, further research is required. Utilising a larger spatial coverage, with more remote locations and a greater temporal coverage can aid with determining the correlation between concentration and proximity to camp.

The relative abundance of polymer types found across sites here are concurrent with those found in other polar environments including glaciers (González-Pleiter et al., 2021), sea-ice (Peeken et al., 2018, Kelly et al., 2020) and sediments (Munari et al., 2017). Polyamide (PA), polyethylene terephthalate (PET), polyester (PE), acrylates and polyurethane, polypropylene (PP) and synthetic rubbers are the major polymers found in the cryosphere, and this is reflected in the samples investigated here. Since cryosphere locations are often remote and far from heavily populated microplastic emission sources, they may also be considered a temporal sink for atmospheric microplastics. These cryospheric regions are consequently critical future study sites for determining temporal fluxes in microplastic pollution. As an example, and preliminary indicator, the concentration of microplastic observed in this study at UG1 represents legacy microplastic from the Union Glacier camp and may be compared with the concentration in "clean snow" to determine the current microplastic footprint at the time of measuring. In the current study, the current footprint 884 (MPL^{-1}) is greater than that observed at depth 150 MPL^{-1} which may indicate an increased plastic footprint to the previous year. The concentrations of every polymer except polypropylene is greater in the current than the legacy sample.

The high abundance of microplastics in Antarctic snow found in this study may have wider climatic and ecological implications. Of particular concern, the light absorbing properties of microplastics have recently been suggested to cause major changes in the albedo of snow and therefore the melt rate of cryospheric regions (Revell et al., 2021; Zhang et al., 2022). The high abundance of microplastics

identified within Antarctic snow in the current study therefore highlights the need for additional work to decipher microplastics influence on snow and ice in these regions. Regarding ecological implications, samples have been collected in areas where strong katabatic winds can redistribute surface snow (Picard et al., 2019; Hoffman et al., 2020) and therefore have the potential to transport microplastics from the near surface, long distances across Antarctica, as recently modelled by Aves et al., (2022). Following the katabatic winds, 86km to the edge of the Ronne Filchner Ice shelf, there exists numerous penguin colonies with stable populations persisting the last 65 years (Orgeira et al., 2021). Microplastics, predominantly PE and PET, have been found in several penguin species, including Gentoo (Bessa et al., 2019), King (Le Guen et al., 2020), Adelie, and Chinstrap (Fragão, et al., 2021). Microplastics released from remote sites could be transported to areas of high ecological importance. Aligned with increasing evidence for uptake by Antarctic biota at different trophic levels (Wilkie Johnston et al., 2023, Fragão, et al., 2021), the findings of the current study suggests that remote camps present a risk of plastic pollution not currently accounted for in the environmental legislation of the region.

In summary, this study shows that regardless of the size of the camp, the presence of humans in Antarctica is leaving a considerable microplastic footprint in the snow, with the concentrations in this study being considerably higher than previously recorded in remote Antarctica (Aves et al., 2022). There is currently no benchmark to determine what this plastic footprint is and whether it varies amongst the size of research bases. Hence, remote camps should be monitored for microplastic pollution and actions to reduce this footprint should be taken. On a broader scale, the findings of this study i.e. high microplastic concentrations at the most remote and sensitive region of earth, magnify the need for collaborative, global plastic pollution mitigation strategies.

Acknowledgement:

K.J.W was supported by Airbnb and knowledges Antarctic Logistics and Expeditions and partners including INACH and Universidad for Magellanes as well as the citizen science group. S.P. was supported under the framework of JPI Oceans by the German Federal Ministry of Education and Research (Project FACTS - Fluxes and Fate of Microplastics in Northern European Waters; BMBF grant 03F0849A) and from the European Union's Horizon 2020 Coordination and Support Action programme under Grant agreement 101003805 (EUROqCHARM). This output reflects only the authors view and the European Union cannot be held responsible for any use that may be made of the information

contained therein. The research falls under the framework of the scotia sea open-ocean observatory (SCOOBIES).

REFERENCES

Allen, S., Allen, D., Phoenix, V.R., Le Roux, G., Durántez Jiménez, P., Simonneau, A., Binet, S., Galop, D., 2019. Atmospheric transport and deposition of microplastics in a remote mountain catchment. Nat. Geosci. 12, 339–344. https://doi.org/10.1038/s41561-019-0335-5

Aves, A.R., Revell, L.E., Gaw, S., Ruffell, H., Schuddeboom, A., Wotherspoon, E., Larue, M., Mcdonald, A.J., 2022. First evidence of microplastics in Antarctic snow. Cryosph. 1–31.

Bergmann, M., Mützel, S., Primpke, S., Tekman, M.B., Trachsel, J., Gerdts, G., 2019. White and wonderful? Microplastics prevail in snow from the Alps to the Arctic. Sci. Adv. 5, eaax1157. https://doi.org/10.1126/sciadv.aax1157

Bessa, F., Ratcliffe, N., Otero, V., Sobral, P., Marques, J.C., Waluda, C.M., Trathan, P.N., Xavier, J.C., 2019. Microplastics in gentoo penguins from the Antarctic region. Sci. Rep. 9, 1–7. https://doi.org/10.1038/s41598-019-50621-2

Brahney, J., Mahowald, N., Prank, M., Cornwell, G., Klimont, Z., Matsui, H., & Prather, K. A. (2021). Constraining the atmospheric limb of the plastic cycle. *Proceedings of the National Academy of Sciences of the United States of America*, *118*(16). https://doi.org/10.1073/PNAS.2020719118/-/DCSUPPLEMENTAL

Cai, M., Yang, H., Xie, Z., Zhao, Z., Wang, F., Lu, Z., Sturm, R., Ebinghaus, R., 2012. Per- and polyfluoroalkyl substances in snow, lake, surface runoff water and coastal seawater in Fildes Peninsula, King George Island, Antarctica. Journal of Hazardous Materials, 209–210, 335-342. https://doi.org/10.1016/j.jhazmat.2012.01.030.

COMNAP., 2022. COMNAP Antarctic Facilities. Available at: COMNAP Antarctic Facilities (arcgis.com) (Accessed: 10 December 2022).

Dris, R., Gasperi, J., Rocher, V., Saad, M., Renault, N., Tassin, B., 2015. Microplastic contamination in an urban area: A case study in Greater Paris. Environ. Chem. 12, 592–599. https://doi.org/10.1071/EN14167

Fragão, J., Bessa, F., Otero, V., Barbosa, A., Sobral, P., Waluda, C.M., Guímaro, H.R. and Xavier, J.C., 2021. Microplastics and other anthropogenic particles in Antarctica: Using penguins as biological samplers. Science of The Total Environment, 788, 147698. https://doi.org/10.1016/j.scitotenv.2021.147698

Fraser, C.I., Kay, G.M., Plessis, M. du, Ryan, P.G., 2016. Breaking down the barrier: dispersal across the Antarctic Polar Front. Ecography (Cop.). 40, 235–237. https://doi.org/10.1111/ecog.02449

Gonzalez-Pleiter, M., Lacerot, G., Edo, C., Pablo Lozoya, J., Leganes, F., Fernandez-Pinas, F., Rosal, R., Teixeira-De-Mello, F., 2021. A pilot study about microplastics and mesoplastics in an Antarctic glacier. Cryosphere 15, 2531–2539. https://doi.org/10.5194/tc-15-2531-2021

Hoffmann, K., Fernandoy, F., Meyer, H., Thomas, E.R., Aliaga, M., Tetzner, D., Freitag, J., Opel, T., Arigony-Neto, J., Florian Göbel, C., Jaña, R., Rodríguez Oroz, D., Tuckwell, R., Ludlow, E., Mcconnell, J.R., Schneider, C., 2020. STable water isotopes and accumulation rates in the Union Glacier region, Ellsworth Mountains, West Antarctica, over the last 35 years. Cryosphere 14, 881–904. https://doi.org/10.5194/tc-14-881-2020

Hoffmann, L., Eggers, S.L., Allhusen, E., Katlein, C., Peeken, I., 2020. Interactions between the ice

algae Fragillariopsis cylindrus and microplastics in sea ice. Environ. Int. 139. https://doi.org/10.1016/j.envint.2020.105697

IAATO. 2021. Tourism Statistics-IAATO. Available at https://iaato.org/tourism-statistics

Kelly, A., Lannuzel, D., Rodemann, T., Meiners, K.M., Auman, H.J., 2020. Microplastic contamination in east Antarctic sea ice. Mar. Pollut. Bull. 154, 111130. https://doi.org/10.1016/j.marpolbul.2020.111130

Long, X., Fu, T. M., Yang, X., Tang, Y., Zheng, Y., Zhu, L., Shen, H., Ye, J., Wang, C., Wang, T., & Li, B. (2021). Efficient Atmospheric Transport of Microplastics over Asia and Adjacent Oceans. *Environmental Science and Technology*, *2022*, 6252. https://doi.org/10.1021/ACS.EST.1C07825/ASSET/IMAGES/LARGE/ES1C07825_0004.JPEG

Brahney, J., Mahowald, N., Prank, M., Cornwell, G., Klimont, Z., Matsui, H., & Prather, K. A. (2021). Constraining the atmospheric limb of the plastic cycle. *Proceedings of the National Academy of Sciences of the United States of America*, *118*(16). https://doi.org/10.1073/PNAS.2020719118/-/DCSUPPLEMENTAL

Long, X., Fu, T. M., Yang, X., Tang, Y., Zheng, Y., Zhu, L., Shen, H., Ye, J., Wang, C., Wang, T., & Li, B. (2021). Efficient Atmospheric Transport of Microplastics over Asia and Adjacent Oceans. *Environmental Science and Technology*, *2022*, 6252. https://doi.org/10.1021/ACS.EST.1C07825/ASSET/IMAGES/LARGE/ES1C07825_0004.JPEG

Ohno, H., & Iizuka, Y. (2023). Microplastics in snow from protected areas in Hokkaido, the northern island of Japan. *Scientific Reports*, *13*(1). https://doi.org/10.1038/S41598-023-37049-5

Padha, S., Kumar, R., Dhar, A., & Sharma, P. (2022). Microplastic pollution in mountain terrains and foothills: A review on source, extraction, and distribution of microplastics in remote areas. *Environmental Research*, *207*, 112232. https://doi.org/10.1016/J.ENVRES.2021.112232

Simon, M., van Alst, N., & Vollertsen, J. (2018). Quantification of microplastic mass and removal rates at wastewater treatment plants applying Focal Plane Array (FPA)-based Fourier Transform Infrared (FT-IR) imaging. *Water Research*, *142*, 1–9. https://doi.org/10.1016/J.WATRES.2018.05.019

Thompson, R. C. (2015). Microplastics in the Marine Environment: Sources, Consequences and Solutions. In *Marine Anthropogenic Litter* (pp. 185–200). Springer International Publishing. https://doi.org/10.1007/978-3-319-16510-3_7

Zalasiewicz, J., Waters, C. N., Ellis, E. C., Head, M. J., Vidas, D., Steffen, W., Thomas, J. A., Horn, E., Summerhayes, C. P., Leinfelder, R., McNeill, J. R., Gałuszka, A., Williams, M., Barnosky, A. D., Richter, D. de B., Gibbard, P. L., Syvitski, J., Jeandel, C., Cearreta, A., … Zinke, J. (2021). The Anthropocene: Comparing Its Meaning in Geology (Chronostratigraphy) with Conceptual Approaches Arising in Other Disciplines. *Earth's Future*, *9*(3), e2020EF001896. https://doi.org/10.1029/2020EF001896

Supplementary Files

This is a list of supplementary files associated with this preprint. Click to download.

- SnowSIsubmission.pdf